Control of floating robots using attractor dynamics[1]

Estela Bicho
Universidade do Minho
Dept. Electronica Industrial
Guimaraes
PORTUGAL
estela.bicho@dei.uminho.pt

Andre Moreira
Universidade do Minho
Dept. Electronica Industrial
Guimaraes
PORTUGAL
amoreira@dei.uminho.pt

Manuel Carvalheira
Universidade do Minho
Dept. Electronica Industrial
Guimaraes
PORTUGAL
mcarvalheira@netcabo.pt

Abstract – **To enable floating robots to autonomously reach for a target position while avoiding obstacles we have generalized the attractor dynamics approach established for wheeled mobile robots to motion generation in blimps or lighter-than-air vehicles. In this approach the level of modelling is at the level of behaviours. A "dynamics" of behaviour is defined over a state space of behavioural variables (heading direction, forward velocity and altitude). The environment is also modelled in these terms by representing task constraints as attractors (i.e. asymptotically stable states) or reppelers (i.e. unstable states) of behavioural dynamics. Attractors and repellers are combined into a vector field that governs the blimp's behaviour. The resulting dynamical systems that generate the flying behaviour is non-linear and presents several attractors and reppelers (typically few) . By design the dynamic systems are tuned so that the behavioural variables are always very close to one attractor. Thus the motion of the airship is controlled by a time series of asymptotically stable states. Computer simulations that integrate the dynamic control architecture and the blimp's physical model indicate that if parameter values are chosen within reasonable ranges, then the over all system works quite well even in cluttered environments. The stability properties of the dynamic control architecture enable the floating robot to remain robust against perturbations.**

I. INTRODUCTION

The challenge to develop autonomous floating robots such as blimps or lighter-than-air vehicles is an important endeavour; the reason is that these airships outperform airplanes and helicopters in tasks that require low-level speed and low altitude. Examples of such tasks are environmental and traffic monitoring, transportation, etc. Thus, many research concentrate their efforts in the development of such robotic systems (e.g. [3],[4],[5],[6],[10],[11], [12])

Here we focus on the control of an autonomous blimp that must fly toward a target destination while avoiding obstacles. Particular to our work, we use non-linear dynamic systems as a theoretical language and framework to design a control architecture that generates the blimp's flying behaviour. Specifically, the time courses of the control variables (i.e. heading direction, forward velocity and altitude) are obtained from a relaxation toward moving attractor solutions of dynamic systems formalized as differential equations. The operation close to attractors guarantees the asymptotic stability of the control systems. Our motivation comes from previous works on wheeled mobile robots which have shown that this theoretical framework can be used to describe the dynamic coupling between the robot and its environment. Additionally in (Iossifidis, Schöner et. al. [7]) has been shown how the attractor dynamics approach can be used for trajectory formation in robot arms.

An open question is to which extend the non-linear attractor dynamics approach can be used to control the behaviour of floating robots (in 3D) which, in contrast to previously used robots that are essentially kinematical systems, exhibit large inertia and thus are highly dynamical systems?

We assume that the floating robot has no apriori' knowledge of the environment and that it acquires sensory information through a colour CMOS camera. Image processing gives the direction, distance and difference in altitude at which target and obstacles are located as seen from the current position of the blimp. Computer simulations that integrate the dynamic control architecture and the blimp's physical model indicate that if parameter values are chosen within reasonable ranges, then the over all system works quite well even in cluttered environments.

The rest of the paper is structured as follows: section II describes the airship physical model and dynamics. Next, section III explains how we use attractor dynamics to generate the airship floating behaviour. Simulation results are presented in section IV. The paper ends with section V with conclusion and an outlook for near future work.

II.AIRSHIP PHYSICAL MODEL

The airship is a balloon in which the lift is independent of flight speed, what is called aerostatic lift.

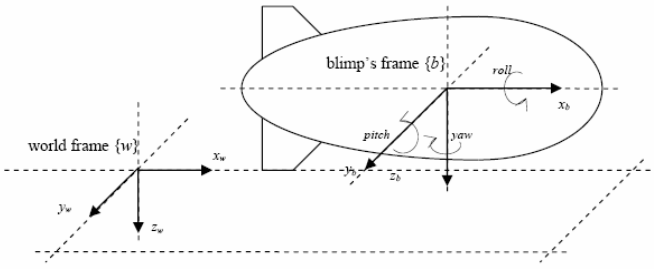

Fig. 1. Airship {b} and world {w} frames

Its model is a state space MIMO with three inputs and eighteen outputs (c.f. (10) and (11)).

[1] This Project was supported, in part, through grant POSI/SRI/38051/2001 to E.B. from the Portuguese Foundation for Science and Technology (FCT) and FEDER.

A Kinematics

The kinematics description of the airship is based in two reference frames, one placed in the airship body {*b*} at the buoyancy centre, and the other in a fixed reference in the ground plane {*w*},

The physical variables that are used to describe the model of the system are:

$$\eta = \left[\eta_1^T, \eta_2^T\right] \text{ where} \tag{1}$$

$$\eta_1^T = \left[x, y, z\right]^T \text{ and } \eta_2^T = \left[\psi, \theta, \phi\right]^T$$

$$\nu = \left[\nu_1^T, \nu_2^T\right] \text{ where} \tag{2}$$

$$\nu_1^T = \left[\nu_x, \nu_y, \nu_z\right]^T \text{ and } \nu_2^T = \left[\omega_x, \omega_y, \omega_z\right]^T$$

$$\tau = \left[\tau_1^T, \tau_2^T\right] \text{ where} \tag{3}$$

$$\tau_1^T = \left[F_x, F_y, F_z\right]^T \text{ and } \tau_2^T = \left[N_x, N_y, N_z\right]^T$$

vector η contains the coordinates of the airship's frame {b} in {w} while ν and τ vector represent the velocities and applied forces, described in {b}. In respect to η_2, ψ is the roll, θ is the pitch and ϕ is the yaw (degrees in rad). As for ω_x, ω_y and ω_z these are respectively the roll rate pitch rate and yaw rate (angular velocity in rad/s). For τ, N_x , N_y and N_z are the torque and F_x, F_y and F_z are the applied forces.

The kinematics equations of the airship in relation to the world are converted by the following Jacobean J_1:

$$\dot{\eta}_1 = J_1(\eta_2)\nu_1 \tag{4}$$

where

$$J_1(\eta_2) = \begin{bmatrix} c\psi c\theta & -s\psi c\theta + c\psi s\theta s\phi & s\psi s\theta + c\psi s\theta c\phi \\ s\psi c\theta & c\psi c\theta + s\psi s\theta s\phi & -c\psi s\theta + s\theta s\psi c\phi \\ -s\theta & c\psi s\phi & c\theta c\phi \end{bmatrix}$$

The velocity in the world is the velocity (ν_x, ν_y, ν_z) multiply by the Jacobean J_2 giving us

$$\dot{\eta}_2 = J_2(\eta_2)\nu_2 \tag{5}$$

$$J_2(\eta_2) = \begin{bmatrix} 1 & s\theta t\theta & c\phi t\theta \\ 0 & c\phi & s\phi \\ 0 & s\phi c\theta & c\phi c\theta \end{bmatrix}$$

$$\begin{bmatrix} \dot{\eta}_1 \\ \dot{\eta}_2 \end{bmatrix} = \begin{bmatrix} J_1 & 0_{[3x3]} \\ 0_{[3x3]} & J_2 \end{bmatrix} \cdot \begin{bmatrix} \nu_1 \\ \nu_2 \end{bmatrix}$$

B Airship Dynamics

The airship dynamics can be written in the form of the following equation, whose variables are described in the frame of airship {*b*}[3].

$$M\dot{\nu}_b + C(\nu_b)\nu_b + D(\nu_b)\nu_b + g(\eta_b) = \tau_b \tag{6}$$

Where ***M*** is the mass matrix (including added mass terms), ***C*** is the Coriolis matrix, ***D*** is the aerodynamic damping, ***g*** is the restoring force (gravity and buoyancy) and **τ** is the actuation forces and torques. The *M* matrix is depicted below:

$$M = \begin{bmatrix} m+a_{11} & 0 & 0 & 0 & m\times z_g & 0 \\ 0 & m+a_{22} & 0 & -m\times z_g & 0 & m\times x_g \\ 0 & 0 & m+a_{33} & 0 & -m\times x_g & 0 \\ 0 & -m\times z_g & 0 & I_{xx}+a_{44} & 0 & 0 \\ m\times z_g & 0 & -m\times x_g & 0 & I_{yy}+a_{55} & 0 \\ 0 & m\times x_g & 0 & 0 & 0 & I_{zz}+a_{66} \end{bmatrix} \tag{7}$$

here *m* is the airship mass, a_{ij} is the added mass matrix terms, I_{ij} are the Inertia coefficient Matrix terms and x_g, y_g and z_g are the coordinates of the centre of mass in relation to the centre of buoyancy [10].

The damping matrix *D* is:

$$D = [D_{V_x} + D_{V_xV_x}|V_x|, D_{V_y} + D_{V_yV_y}|V_y|, D_{V_z} + D_{V_zV_z}|V_z|, \\ D_{\omega_x} + D_{\omega_x\omega_x}|\omega_x|, D_{\omega_y} + D_{\omega_y\omega_y}|\omega_y|, D_{\omega_z} + D_{\omega_z\omega_z}|\omega_z|] \tag{8}$$

$$g(\eta_b) = \begin{bmatrix} [0]_{3\times1} \\ -m\times g\times\cos(\theta)\times\sin(\psi)\times y_g + m\times g\times\cos(\theta)\times\sin(\psi)\times z_G \\ -m\times g\times\sin(\theta)\times z_g + m\times g\times\cos(\theta)\times\cos(\psi)\times x_G \\ -m\times g\times\cos(\theta)\times\sin(\psi)\times x_g + m\times g\times\sin(\theta)\times y_G \end{bmatrix} \tag{9}$$

This matrix terms are self explaining, but if you wish to further explore these items please check [3].

We assume that the airship is moving slowly, being so the Coriolis matrix is considered null and the airship model can be approximated to:

$$\dot{x}_{xy} = \begin{bmatrix} -M_{xy}^{-1}D_{xy} & -M_{xy}^{-1}g_{xy} \\ J_{xy} & [0]_{3x3} \end{bmatrix} x_{xy} + \begin{bmatrix} M_{xy}^{-1}B_{xy} \\ [0]_{3x2} \end{bmatrix} u_{xy} \tag{10}$$

$$\dot{x}_{xz} = \begin{bmatrix} -M_{xz}^{-1}D_{xz} & -M_{xz}^{-1}g_{xz} \\ J_{xz} & [0]_{3x3} \end{bmatrix} x_{xz} + \begin{bmatrix} M_{xz}^{-1}B_{xz} \\ [0]_{3x2} \end{bmatrix} u_{xz} \tag{11}$$

The general mass matrix is simplified for the xy and an xz system, the same is true for the entire matrix presented in the above systems.

The perturbed state variables for the heading direction (xy) matrix are $\boldsymbol{x_{xy}} = [v_y(t)\ \omega_x(t)\ \omega_z(t)\ y(t)\ \psi(t)\ \phi(t)]^T$ and the system input is $u_{xy} = F_y$; For the xz matrix $\boldsymbol{x_{xz}} = [v_x(t)\ v_z(t)\ \omega_x(t)\ x(t)\ z(t)\ \theta(t)]^T$ and $u_{xz} = [F_x\ F_z]^T$.

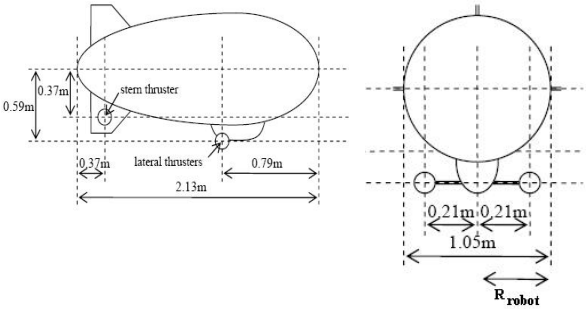

Fig. 2. Airship dimensions

III. BEHAVIOURAL DYNAMICS

To generate the floating behaviour we use the heading direction ϕ, forward velocity, v_b and altitude $\boldsymbol{z}$ as behavioural variables.

A Attractor dynamics for heading direction

A solution for the heading direction dynamics has been previously designed and implemented on wheeled mobile robots (see [1], [2], [8], [9], for details). Here we extend that previous solution to the control of the blimp's heading direction.

As is illustrated in Fig. 3, the direction, ψ_{tar}, in which a target lies as seen from the current position of the blimp in the *xy* plane, specifies a desired value for the heading direction. Directions, ψ_{obsi} in which obstacles are seen specify values of heading direction that must be avoided. A simple dynamical system that generates orientation toward the target direction is

$$\frac{d\phi}{dt} = f_{tar}(\phi) = -\lambda_{tar} \sin(\phi - \psi_{tar}) \tag{12}$$

This creates an attractor (asymptotically stable state) at the direction of the target with rate of relaxation λ_{tar}.
When the blimps floats must not collide with obstacles sensed in the plane *xy* plane at its flying altitude. A dynamical system that generates obstacle avoidance is

$$\frac{d\phi}{dt} = F_{obs}(\phi) = \sum_{i=1}^{n} f_{obs,i}(\phi), \; i = 1,2,3,\ldots n \tag{13}$$

where,

$$f_{obs,i}(\phi) = \lambda_i (\phi - \psi_{obs,i}) e^{-\frac{(\phi-\psi_{obs,i})^2}{2\sigma_i^2}}, \; i = 1,2,3,\ldots n \tag{14}$$

here each term creates a repeller, i.e. unstable state, at the direction, ψ_{obsi}, at which the obstacle is seen. The strength of repulsion, λ_i, of each contribution is a decreasing function of the computed distance:

$$\lambda_i = \beta_1 e^{-\frac{d_i}{\beta_2}} \tag{15}$$

that depends on two parameters controlling overall strength β_1 and spatial rate of decay β_2.

The angular range over which the contribution exerts its repulsive effect is adjusted taking both the angular size of the object, $\Delta\theta$, and an additional angle required for the blimp to pass next to the obstacle at a minimal allowed distance (see Fig.3).

$$\sigma_i = \text{atan}\left(\tan\left(\frac{\Delta\theta}{2}\right) + \frac{R_{robot}}{R_{robot} + d_i} \right) \tag{16}$$

The complete heading direction dynamics is the sum over the above described contributions:

$$\frac{d\phi}{dt} = f_{tar}(\phi) + F_{obs}(\phi) + f_{stoch} \tag{17}$$

The added term f_{stoch} is a stochastic force that ensures escape from repellers when bifurcations in the dynamics take place and, simultaneously, models perturbations.

This superposition is a non-linear dynamical system, which may have multiple attractors and repellers (typically few). By design the system is tuned so that the heading direction is in a resulting attractor of this dynamics most of the time (c.f. Section IV).

Very important, the differences $\phi - \psi_{tar} = \theta_{tar}$, $\phi - \psi_{obsi} = \theta_{obsi}$ in (12) and (13) respectively, are directly given by the vision system (See Fig. 3). This renders the performance independent of the calibration of the planning coordinate system.

Equation (17) determines directly the reference value for the blimp's angular velocity ω_z .

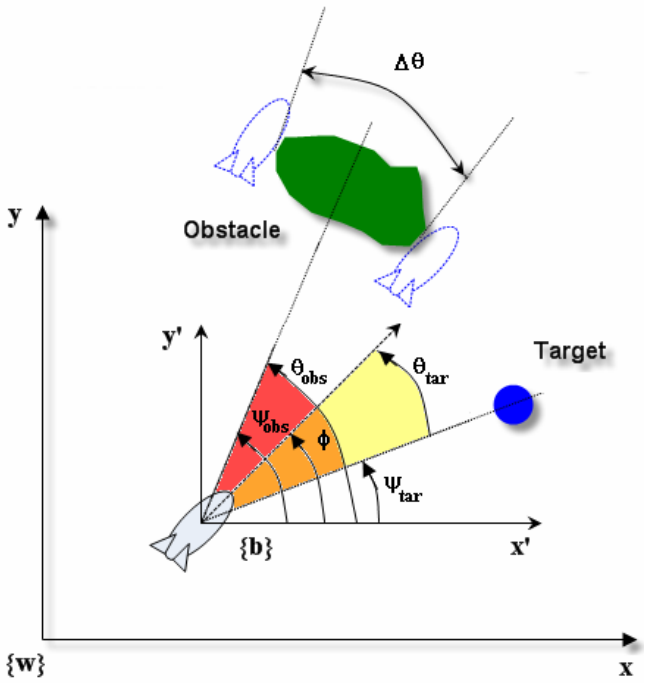

Fig. 3 Constraints and parameters for the airship heading direction dynamics.

B Control of altitude and forward velocity

The control of the forward velocity and altitude is implemented with the following simple linear attractor dynamics:

$$\frac{dz}{dt} = -\lambda_z (z - z_{tar}) \tag{18}$$

$$\frac{dv_b}{dt} = -\lambda_v (v_b - v_{desired}) \tag{19}$$

where Z_{tar} is the target's altitude and defines the desired

value for the blimp's altitude. The difference Z_{robot}-Z_{tar}=ΔZ_{tar} is computed from the image acquired by the vision system.
If no obstacles are seen in the image then the desired forward velocity is v_{tar}, otherwise, if obstacles are sensed then the desired value forward velocity is v_{obs}:

$$v_{desired} = \begin{cases} v_{obs} = \zeta_2 e^{-\frac{\xi_3}{d2o}}, \text{ obstacles dominate} \\ v_{tar} = \frac{1}{\theta_{tar}} e^{-\frac{\xi_1}{d2t}}, \text{ else} \end{cases} \quad (20)$$

where $1/\theta_{tar}$ is a dynamic gain, ξ_1 and ξ_3 are constant parameters, ξ_2 is a static gain, d2t is the distance to the target and d2o is the distance to the nearest obstacle in front of the airship.

The airship model includes two thrusters (portside and starboard) that are capable of directing the thrust ±90º, making the airship go up or down obliquely.

To model this v_b is decomposed into v_x and v_z. The angle of inclination of the thrusters is γ so v_x and v_z are functions of γ.

$$\begin{cases} v_x = v_b \cos(\gamma) \\ v_z = v_b \sin(\gamma) \end{cases} \quad (21)$$

IV. RESULTS

The complete dynamic architecture was evaluated in computer simulations. These were generated by a software simulator written in MATLAB. We modelled the blimp based on its physical model and dynamics. The blimp is a 2,3m airship from Blimpguys inc. Canada. This airship is capable only of indoor flying and is an adequate platform for our implementation. The physical model that was used is an accurate depiction of this airship.
All behavioural related differential equations (Eq. (12), (13) and (17)) are integrated with a forward Euler method. The airship physical model was integrated onto the simulator using Matlab Simulink models that implemented eq. (10) and (11) for heading (x0y) and translational / altitude control (x0z) system. Sensory information is computed once per each cycle and simulates the information given by the vision system (i.e. θ_{tar}, θ_{obsi}, d_{obsi}, ΔZ_{tar}).

A simulation run in a complex scenario which demonstrates several features of the dynamic control architecture is presented in Figs.4 and 5. Fig. 4 shows a 3D view of the airship flying toward the target while simultaneously avoiding obstacles sensed at its altitude.
Fig. 5 shows the corresponding top view and the heading direction dynamics at the points showed in snapshots A-E. The vector fields of the heading direction dynamics change in time due to varying sensory information as the blimps floats. Thus the resultant attractors (i.e. asymptotic stable states shift) shift pulling the heading direction along, i.e. the blimp's heading direction is always relaxing to and following very closely one of the resultant attractors. This contributes to the reinforcement of the asymptotic stability of the system and makes the blimp's behaviour more robust against perturbations.

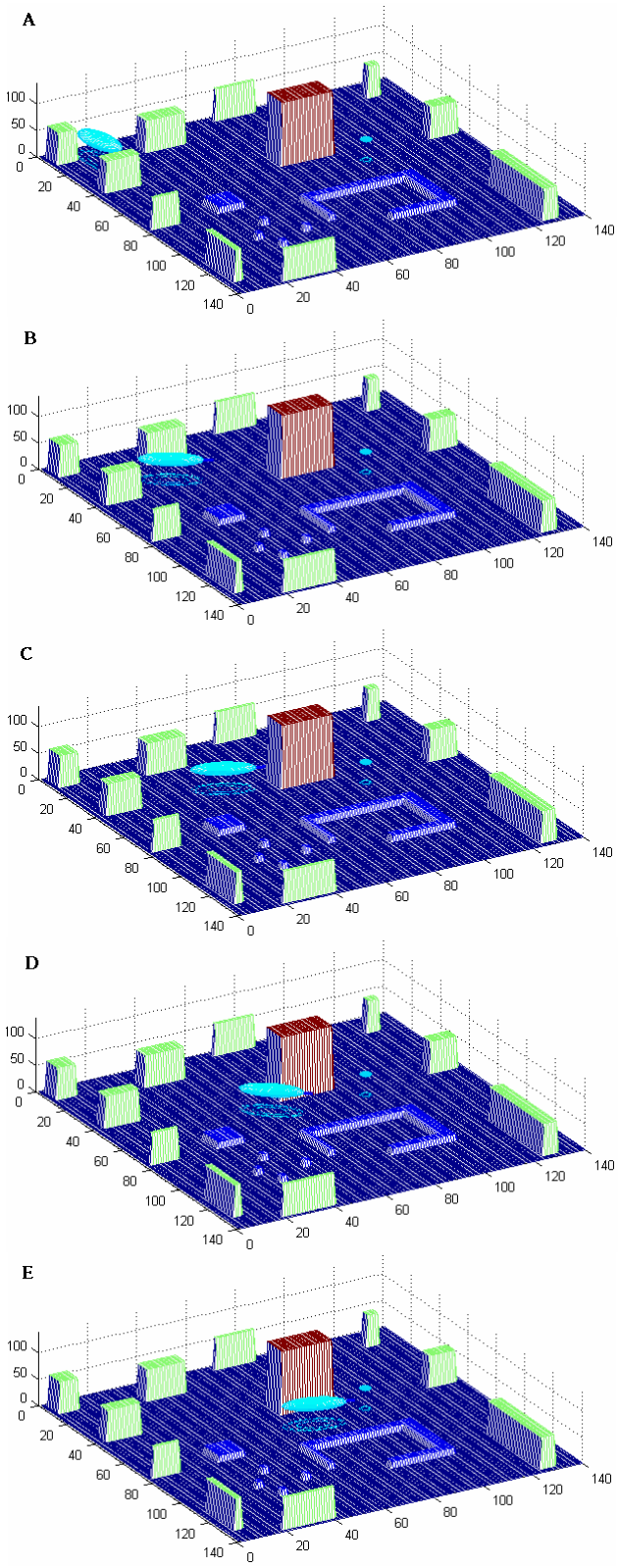

Fig.4. Snapshots of a simulation run of the complete system. The target location is indicated by the small sphere. The airship is represented by an ellipsoid with a (blue) line indicating its heading

direction. Initially the robot is placed as indicated in Panel A at the altitude of the target. The airship moves toward the target location and simultaneously avoids the brown obstacle (Panels B-E). see videos in http://www.dei.uminho.pt/pessoas/estela)

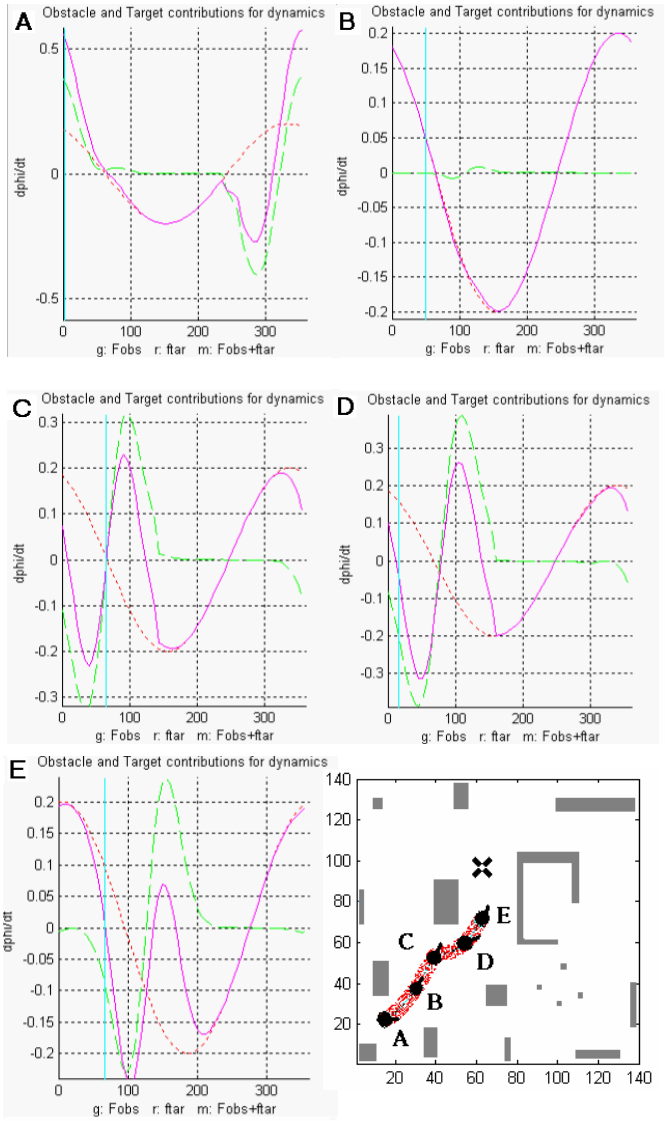

Fig. 5. Internal heading direction dynamics at positions depicted in snapshots A-E in Fig.4. the dashed green line and red dotted line represent the obstacle avoidance target contributions for the dynamics respectively. The solid magenta solid line is the complete dynamics (the sum of the other two). The vertical cyan line represents the airships current heading direction at the instant of the snapshot. The final panel is the 2D view of the simulation shown in Fig. 4. The resultant dynamics exhibit several attractors (i.e. zero crossing with negative slope) repellers (i.e. zero crossing with positive slope). From panel A to E we can see that as sensory information changes the resultant attractors and repellers change. The blimp's heading direction is always very close to one of the resultant attractors and follows the attractor as it shifts due to changing sensory information.

A second simulation run that challenges the airship behaviour in a cluttered environment is shown in Fig. 6.

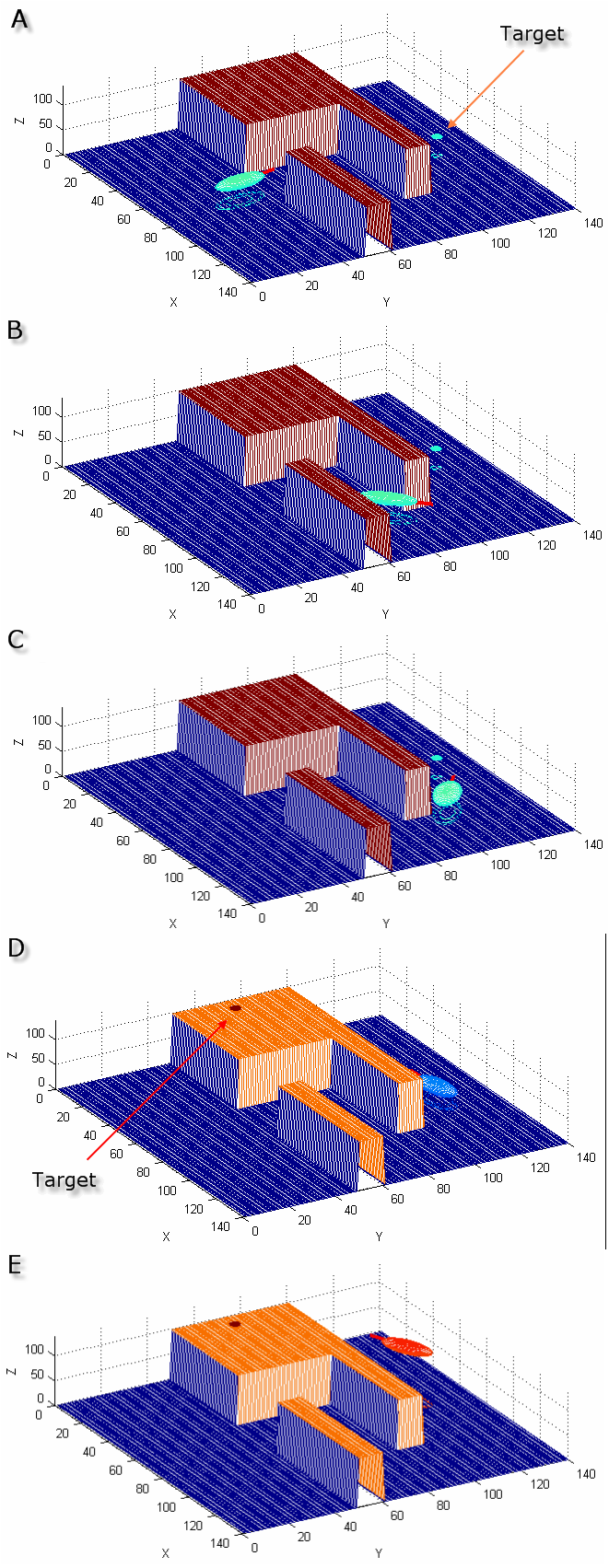

F

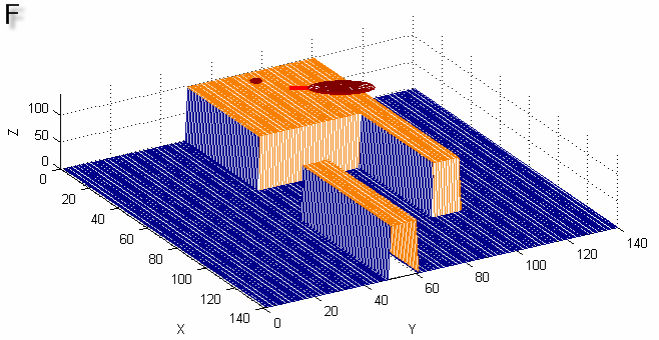

Fig. 6 Snapshots of a simulation run with a narrow passage for the airship. The robot starts as depicted in panel A and the target is initially at the position indicated in this panel. The airship smoothly floats along the "L" shape passage and as one can see successfully avoids collisions with the walls and first target location (Panels A-D). When the airship reaches the target position the target is shifted to the position indicated in panel D. The airship increases its altitude and simultaneously turn toward the new target location and avoids collisions with the obstacle (Panels D-E). (see videos in http://www.dei.uminho.pt/pessoas/estela)

V. DISCUSSION AND CONCLUSIONS

We have demonstrated that non-linear attractor dynamics can be used to control the behaviour of floating robots (in 3D) which, in contrast to previously used wheeled mobile robots exhibit large inertia and thus are highly dynamical and perturbable systems. The airship has no prior knowledge of the environment. Motion is generated by a time series of attractor solutions. Computer simulations that integrate the dynamic control architecture and the blimp's physical model indicate that if parameter values are chosen within reasonable ranges, then the over all system works quite well even in cluttered environments. The stability properties of the dynamic control architecture enable the floating robot to remain robust against perturbations.

Although the airship physical model was used for simulation purposes, that information is not necessary for the dynamic control architecture that generates the floating behaviour. This is important because it simplifies the design dynamic control architecture.

The work described here imposes of course further research. The next logical step is the physical implementation of the dynamic control architecture on the platform (2,3m airship from Blimpguys inc. Canada). This implementation is being done as we speak and we hope to be able to show results in the near future.

VI ACKNOWLEDGMENT

We are very grateful to Nzoji Hipolito, Luis Louro, Sergio Monteiro, Carlos Gregorio and Marta Silva for their motivation and help in many ways.

VII REFERENCES

[1] E. Bicho and G. Schoner, "Target Position Estimation, Target acquisition and Obstacle Avoidance", in *Proceedings of the IEEE International Symposium on Industrial Electronics* (ISIE'97), pages SS13-SS20, IEEE, Piscataway, N.J. 1997.

[2] E. Bicho, "*Dynamic approach to behavior-based robotics: design, specification, analysis, simulation and implementation*", Shaker Verlag, Aachen, 2000, ISBN 3-8265-7462-1

[3]A. Elfes, S.S. Bueno, M. Bergerman, J.G. Ramos, and S.B Varella Gomes, "Project AURORA: development of an autonomous unmanned remote monitoring robotic airship". Journal of the Brazilian Computer Society, 4(3), pp 70--78, April 1998.

[4] A. Elfes, S. S. Bueno, M. Bergerman, and J. J. G. Ramos. "A semi-autonomous robotic airship for environmental monitoring mission", in *Proceedings of the IEEE International Conference on Robotics and Automation*, Leuven, Belgium, May 1998, pp 3449--3455, 1998.

[5] S.B.V Gomes, "*An investigation of the flight dynamics of airships with application to the YEZ-2A*", PhD Thesis, College of Aeronautics, Cranfield University, October 1990.

[6] S.B.V. Gomes and J.J.G. Ramos, "Airship dynamic modelling for autonomous operation", in *Proceedings of the IEEE International Conference on Robotics and Automation*, Leuven, Belgium, pp 3462-3467, May 1998.

[7] I. Iossifidis and G. Schöner, "Autonomous reaching and obstacle avoidance with the anthropomorphic arm of a robotic assistant using the attractor dynamics approach", in *Proceedings of the IEEE 2004 International Conference On Robotics and Automation*, New Orleans, USA, April 26 - May 1 2004.

[8]A Steinhage. *Dynamical Systems for the Generation of Navigation Behavior*. Shaker Verlag, Aachen, 1998.

[9] G Schoner, M Dose, and C Engels. Dynamics of behavior: Theory and applications for autonomous robot architectures. *Robotics and Autonomous Systems*, 16:213–245, 1995.

[10] J. Santos Victor, M.F. Metelo, L.R. Campos, "Vision Based Control of an Autonomous Blimp", ISR-IST, September 2003.

[11] H. Zhang, J.P. Ostrowski, "Visual servoing with dynamics: Control of an unmanned blimp", in *Proceedings of the IEEE International Conference on Robotics and Automation*, Detroit, MI, May 1999.

[12] H.Zhang and J.P Ostrowski. "*Visual servoing with dynamics: Control of an unmanned blimp (Technical report)",* General Robotics, Automation, Sensing and Perception laboratory (GRASP), University of Pennsylvania, 1998.